

Portland State University PDXScholar

Geology Faculty Publications and Presentations

Geology

2013

Strain Energy Release from the 2011 9.0 Mw Tōhoku Earthquake, Japan

Kenneth M. Cruikshank

Portland State University

Curt D. Peterson

Portland State University, petersonc@pdx.edu

Let us know how access to this document benefits you.

Follow this and additional works at: https://pdxscholar.library.pdx.edu/geology_fac



Part of the [Geology Commons](#), and the [Tectonics and Structure Commons](#)

Citation Details

Cruikshank, K. M., & Peterson, C. D. (2013). Strain Energy Release from the 2011 9.0 Mw Tōhoku Earthquake, Japan. *Open Journal of Earthquake Research*, 2013.

This Article is brought to you for free and open access. It has been accepted for inclusion in Geology Faculty Publications and Presentations by an authorized administrator of PDXScholar. For more information, please contact pdxscholar@pdx.edu.

Strain Energy Release from the 2011 9.0 M_w Tōhoku Earthquake, Japan

Kenneth M. Cruikshank, Curt D. Peterson

Department of Geology, Portland State University, Portland, USA
Email: CruikshankK@pdx.edu, PetersonC@pdx.edu

Received September 15, 2013; revised October 17, 2013; accepted October 31, 2013

Copyright © 2013 Kenneth M. Cruikshank, Curt D. Peterson. This is an open access article distributed under the Creative Commons Attribution License, which permits unrestricted use, distribution, and reproduction in any medium, provided the original work is properly cited.

ABSTRACT

The purpose of this paper is to compare the strain energy released due to elastic rebound of the crust from the tragic 2011 9.0 M_w Tōhoku earthquake in Japan with the observed radiated seismic energy. The strain energy was calculated by analyzing coseismic displacements of 1024 GPS stations of the Japanese GEONET network. The value of energy released from the analysis is 1.75×10^{17} J, which is of the same order of magnitude as the USGS-observed radiated seismic energy of 1.9×10^{17} Nm (J). The strain energy method is independent of seismic methods for determining the energy released during a large earthquake. The analysis shows that although the energy release is concentrated in the epicentral region, about 12% of the total energy was released throughout the Japanese islands at distances greater than 500 km west of the epicenter. Our results also show that outside the epicentral region, the strain-energy was concentrated along known tectonic zones throughout Japan.

Keywords: Japan; Earthquake; Crustal Strain; GPS; Radiated Energy

1. Introduction

Reid's [1] elastic rebound theory indicates that an understanding of the pattern and magnitude of strain in the loading phase of the earthquake cycle is important for evaluating the seismic risk in an area. Some insights into the strain patterns in the loading phase can be gained by examining the pattern of strain in the unloading or earthquake phase. Measurements of tectonic strain release during the 2011 Tōhoku earthquake and tsunami [2] (**Figure 1**) provide important insights into the mechanisms of subduction zone earthquakes. These relations should be of use in other subduction zones where modern strain records might help to constrain predictions of earthquake strain release and energy. To our knowledge, these are the first wide-field comparisons of radiated energy and observed strain energy reported for a subduction zone.

Analysis of strain energy provides a method for estimating the total energy released without assuming a particular earthquake mechanism. For example, estimates of the energy from an earthquake using either the Scalar Moment or Observed Radiated Energy are often different by 5 to 6 orders of magnitude, with the seismic moment being substantially larger than the observed radiated energy [e.g., 3, Figure 12]. (Although, it should be noted

that the seismic moment is not a direct measure of the energy released in an earthquake, so it will have a value substantially different from the radiated energy [4]). Direct measure of the strain between points on Earth's surface can be calculated from the relative displacement of Global Positioning System (GPS) stations. GPS measurements of crustal strain provide constraints on the distribution of energy release that are not directly available from seismic stations alone.

In this paper we document the regional distribution of coseismic strain in the upper plate from the 2011 Tōhoku earthquake using length-changes between GPS stations in the Japanese GPS network (GEONET, **Figure 2**). Our estimate of the total strain-energy release, 1.75×10^{17} J, is of the same order of magnitude as the observed radiated seismic energy, 1.9×10^{17} J [2]. Our results also show that a portion of the strain-energy was concentrated along known tectonic zones throughout Japan (compare **Figures 1** and **3**). These tectonic zones apparently served as strain concentrators prior to the 2011 earthquake [5]. The distribution of strain release immediately following the 2011 Tōhoku earthquake is generally consistent with reported patterns of strain accumulation that have been observed over the last 50 years [5,6].

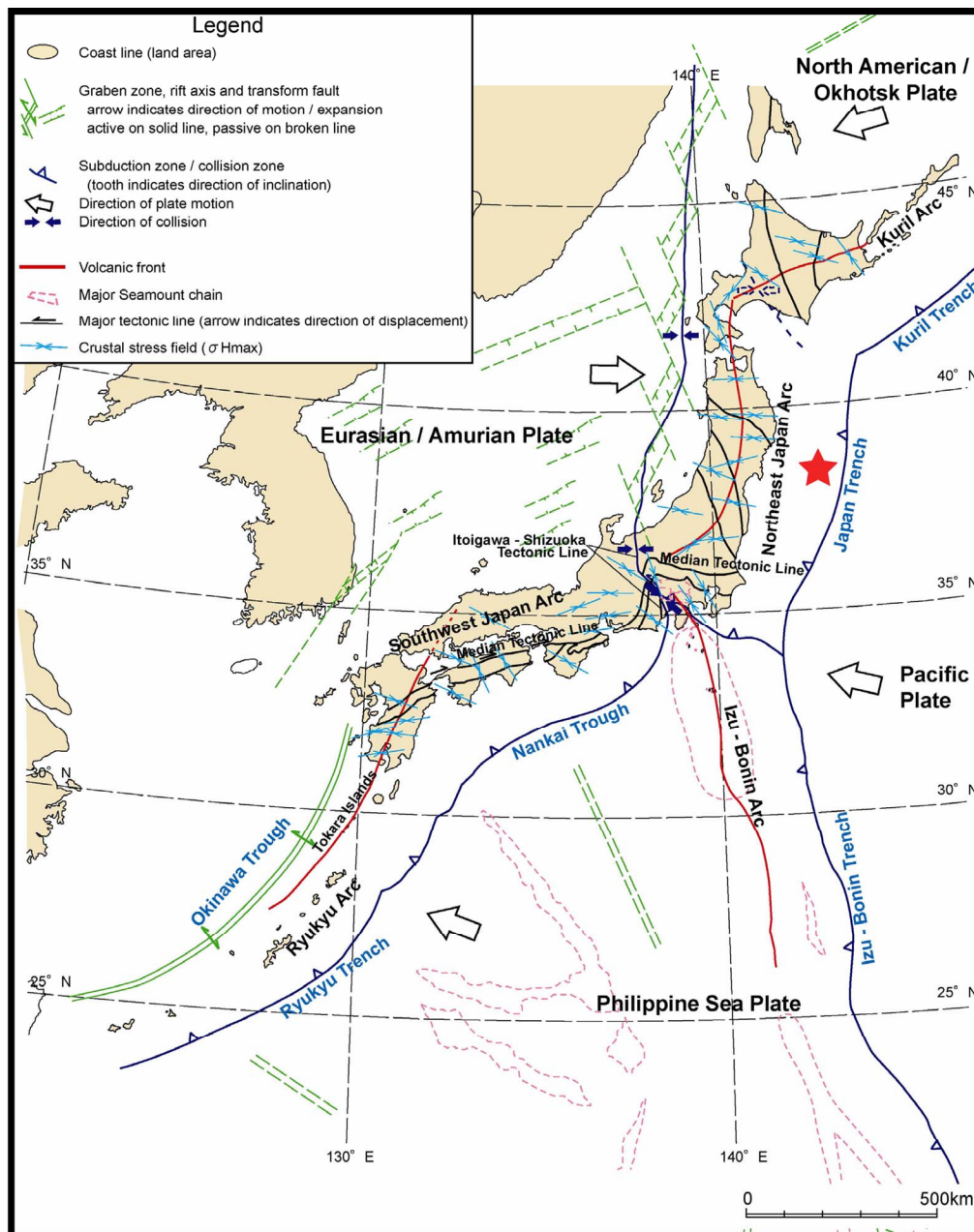


Figure 1. Map showing the current tectonic setting of Japan [Figure 6-2 from 7]. The 2011 epicenter, marked by a red star, is located along the Japan Trench and the Northeast Japan Arc.

2. Background

The energy released in an earthquake is generally believed to come from the release of energy stored by the elastic component of strain in the crust. This is the idea expressed in Reid's elastic rebound theory [1]:

"We know that the displacements which took place near the fault-line occurred suddenly, and it is a matter of much interest to determine what was the origin of the forces which could act in this way. Gravity can not be invoked as the direct cause, for the movements were

practically horizontal; the only other forces strong enough to bring about such sudden displacement are elastic forces. These forces could not have been brought into play suddenly and have set up an elastic distortion; but external forces must have produced an elastic strain in the region about the fault-line, and the stresses this induced were the forces which caused the sudden displacements, or elastic rebounds, when the rupture occurred".

A similar mechanism is used to describe the release of energy in phenomenon such as "rock bursts" in mines [8].

Here we consider the general energy balance for the change in shape of an elastic material. We are not concerned with any particular mechanism.

2.1. Energy Stored in Elastic Deformations

An elastic material is one where the original shape (the unstrained state) will be restored after the forces causing a change in shape (strain) are removed. An elastic material can be thought of as a coiled spring, a spring that resists both being shortened and lengthened. The resistance of the spring to a change in length is the spring constant; we take the value of the spring constant to be the same for both shortening and extension, and the relationship force and change in length is described using Hooke's Law,

$$F = k\Delta L,$$

where F is the force, k the "spring" constant, and ΔL the change in length.

An elastic bar can be shortened by compressing it from either end. The force does work in shortening the bar (and so is using energy). Some of the energy may go into heat generation or permanent shape changes but the recoverable energy which we are interested in will be stored in the "springiness" of the elastic bar. Thus, the result of the change in length of the bar is net-energy "storage" in the bar; this is the *elastic strain energy*. A material will show elastic behavior as long as the length change is small compared to the length of the bar, generally less than 10^{-6} of the length of the bar.

In an elastic material the change in length is reversible once the applied forces are removed (unloaded). When the forces are removed from a bar it attempts to return to its original length. The material may not completely revert to its original geometry, since some of the potential energy has been converted to kinetic energy and heat. If removal of the forces is a very slow process the kinetic energy is negligible. If the removal of the forces is rapid in addition to doing work to restore the material's shape a portion of the stored potential energy will be converted to kinetic energy which will be released as seismic waves.

Short term coseismic changes in length are an effect of the elastic behavior of the rock, not the long-term deformation, thus the *elastic strain energy* represents the maximum potential energy that is available to be transferred to kinetic energy and observed as seismic waves.

In summary, the maximum amount of stored potential elastic energy between two points in an elastic material is proportional to change in distance between those two points and the spring constant of the material. Using GPS the change in distance between two points can be determined, which will then be proportional to the change in elastic potential energy between the two points. This change in elastic potential energy is the maximum

amount of energy that is available to be released as kinetic energy (*i.e.*, seismic waves).

2.2. Strain and Strain Energy

Strain, ϵ , is the normalized change in length of a line between two material points

$$\text{Strain} = (\text{Final Length} - \text{Initial Length}) / \text{Initial Length}$$

$$\text{Strain} = (\text{Change in Length}) / \text{Initial Length}$$

or

$$\text{Strain} = \text{Stretch} - 1$$

where

$$\text{Stretch} = \text{Final Length} / \text{Initial Length}$$

Strain, ϵ , will be negative if the distance between two points gets shorter (shortening), positive if the distance increases (extension), and zero if it is unchanged. The stretch (or stretch ratio), S , will be less than one for shortening, greater than one for extension, and one for no length change.

Over an area, strain (or stretch) provides a description of deformation. This would consist of a series of strains in different directions. Usually the strain is described with two principle components. If we know the principle components and their direction, we can describe the strain in any arbitrary orientation.

Once the principle strains ($\epsilon_1, \epsilon_2, \epsilon_3$) are known, the elastic strain energy is given by [8]:

$$e = \frac{1}{2} \left[\lambda (\epsilon_1 + \epsilon_2 + \epsilon_3)^2 + 2G (\epsilon_1^2 + \epsilon_2^2 + \epsilon_3^2) \right] \quad (1)$$

where

$$G = \frac{E}{2(1+\nu)} \quad \text{and} \quad \lambda = \frac{E\nu}{(1+\nu)(1-2\nu)},$$

where E is Young's Modulus and ν is Poisson's Ratio.

In order to determine the principle strains we need the strain in three different directions. The principle component we end up with will represent some average strain over the region enclosed by the three lines needed for the solution.

GEONET stations were grouped into triangles, and changes in position of the vertices were used to determine the magnitude of the principle strains (the solution also gives the orientations, but that information is not needed for this analysis). If we have three points, we can define a triangle.

Consider a plane triangle, the Euclidian distance is:

$$\text{Distance} = \sqrt{dE^2 + dN^2 + dZ^2}$$

$$\text{Direction } (\theta_{\text{base}}) = \tan^{-1} \left(\frac{dE}{dN} \right)$$

where $dE = (E_A - E_B)$, $dN = (N_A - N_B)$, $dZ = (Z_A - Z_B)$.

If the direction is needed to be converted to an Azimuth (ϕ)

$$\phi = \begin{cases} \text{if } 0^\circ < \theta \leq 90^\circ; 90^\circ - \theta \\ \text{if } 90^\circ < \theta < 360^\circ; 450^\circ - \theta. \end{cases}$$

Knowing the coordinates of A , B and C , the distances between points can be determined. The direction of each line element can also be determined.

Given displacements, dX and dY , the change of line length can be determined, allowing the strain of each line segment to be determined. The displacement vector will not always be parallel to the line segment, so we need to get the component of the net displacement (imagine point A is now fixed, so we look at the relative movement of point B with respect to point A):

$$\begin{aligned} \delta N &= \delta N_A - \delta N_B \\ \delta E &= \delta E_A - \delta E_B \\ \delta Z &= \delta Z_A - \delta Z_B. \end{aligned}$$

This describes a net displacement vector with an orientation of

$$(\theta_{disp}) = \tan^{-1} \left(\frac{\delta E}{\delta N} \right),$$

and magnitude $\sqrt{dE^2 + dN^2 + dZ^2}$. The projection of this vector into the direction of the line segment (θ_{base}) is accomplished by:

$$\text{Angle} = \theta_{disp} - \theta_{base} + \pi$$

$$\delta L = \sqrt{\delta E^2 + \delta N^2 + \delta Z^2} \cos(\text{Angle})$$

to get the change in the vector direction of the line, or the strain between the two stations

Since we are dealing with Geographic Coordinates, the distance and line direction are determined using a modified Vincenty solution [9].

Evaluation of the strain energy (Equation (1)) requires that the principal strains (ϵ_i) are known. Displacements of GPS stations that comprise the 3 vertices of triangles in the GEONET array provide sufficient information to calculate the principal strains within the triangle [e.g., 10, 11]. The basic equations solved are (for irrotational strain, [12]):

$$\begin{aligned} S &= 1 + \epsilon \\ &= \frac{D}{\left[\frac{\partial y}{\partial Y} \cos \theta - \frac{\partial x}{\partial Y} \sin \theta \right]^2 + \left[\frac{\partial x}{\partial X} \sin \theta - \frac{\partial y}{\partial X} \cos \theta \right]^2} \quad (2a) \end{aligned}$$

where

$$D = (\partial x / \partial X)(\partial y / \partial Y) - (\partial x / \partial Y)(\partial y / \partial X). \quad (2b)$$

S is stretch, and θ is the direction cosine for the line,

$\partial x / \partial X$, $\partial y / \partial Y$, $\partial x / \partial Y$, and $\partial y / \partial X$ are components of the deformation gradient tensor [11,13]. Strain is

$$\epsilon_i = S_i - 1. \quad (2c)$$

Equations (2) are solved using displacements of three GPS stations that make up the triangles shown in **Figure 2**; the evaluation of Equation (1) provides the strain energy density for the triangle. Using an average crustal thickness, the total energy changes in the triangular prism can be calculated.

From the principal strains, the average strain energy density can be computed for a given area, assuming values of Young's modulus (E) and Poisson's ratio (ν). We use Hanks and Kanamori [14] typical crustal values of 70 GPa and 0.25 respectively. In this paper we use an average crustal thickness of 30 km based on the USGS CRUST 5.1 model [15] for the Japan region. Variations in the value for average thickness do not significantly change the results of estimated energy release (see Discussion).

2.3. Interpreting the "Total Energy Available" Result

The results from Japan show that coseismic displacements produce areas of shortening and areas of extension. Since the elastic response makes no distinction between energy released by the bar restoring to a longer or shorter dimension, we take all of the areas to be generating potential seismic energy.

Another extreme is to consider only areas extending to be releasing stored energy, and area that are shortening to be "absorbing" energy (although there is no *a priori* basis for assuming this). If we do this, then the result is different by 24% from the assumption for all areas releasing energy. The order-of magnitude of the energy released is the same (10^{17}). We will use the all-cells releasing energy figure, since that would represent the upper-limit of available energy, although it is possible that about 12% goes into "loading" other areas of the crust during the earthquake.

3. Data and Methods

The Japanese nation-wide dense GPS network (GEONET, **Figure 2**) has been in operation since 1996 [5]. In this paper we only use displacements recorded in the 9 minutes following the March 2011 Tōhoku earthquake (**Figure 1**). This allows us to exclude any movement from aftershocks. The relative displacement of the GPS stations represents the change in crustal strain. According to Reid's [1] elastic rebound theory the change in strain represents stored elastic energy that is available to be released as seismic waves.

Many of the 1024 stations in GEONET range from 20

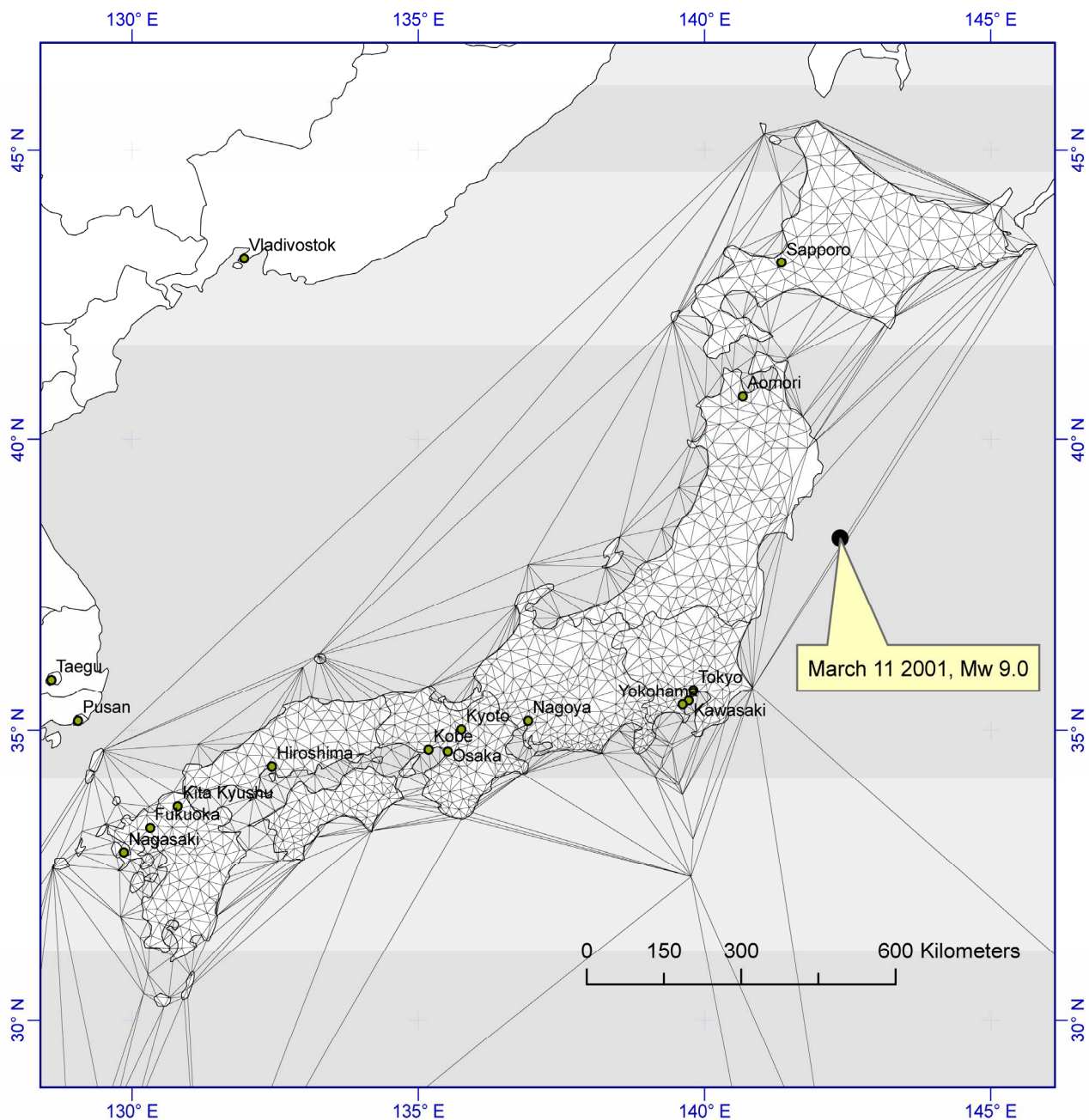


Figure 2. GPS stations that comprise the Japanese GEONET network and the Delauney Triangles that were formed using the 1024 GPS stations. Principal strains for each triangle are calculated, from which the strain energy density for each triangle is computed. The location of the March 2011 M_w 9.0 earthquake is shown on the NE coast of Honshu.

to 40 km apart (**Figure 2**) and provide data coverage up to 1500 km from the 2011 epicenter. A network of 2393 triangles has been used to look at strain accumulation over the last decade [e.g., 16]. Several stations are on islands (**Figure 2**), thus strain in the oceanic crust to the east of Japan can also be calculated, although at lower resolution because of the increased distance between GPS stations. We use the displacement of these stations to calculate the energy released from stored elastic strain

as well as the distribution of energy release. This data provides insight where strain energy was released or stored following an earthquake, without the need to assume a particular deformation model, e.g., displacement discontinuities on a fault. GPS gives maps of coseismic displacements that cannot be obtained from traditional re-surveying of control networks that may take years [e.g., 17,18] during which time additional displacements may occur.

Data from GEONET was processed by the Advanced Rapid Imaging and Analysis (ARIA) [19] team at JPL/California Institute of Technology. Version 0.3 of the processed data consisted of coseismic displacements estimated from 5-minute interval kinematic solutions. The coseismic displacements are the difference between the solutions at 5:40 UTC and at 5:55 UTC. The earthquake occurred at 05:46 UTC, starting the 9 minute period of strain measurements. Using this time frame minimizes displacements from aftershocks and other unrelated events. A search of the IRIS database (IRIS, 2011) for the region bounded by 128° to 146° E, 29° to 46° N and the GPS time frame found only the main shock (**Figure 2**). The following steps were taken:

Stations were grouped to form non-overlapping triangles (**Figure 2**) [e.g., 20].

The initial latitude-longitude positions were used to calculate the initial length (l_i) and direction (θ_i) for each side in each triangle.

The displacements at each vertex in a triangle were used to determine the final length of each side of the triangle (L_i). The triangles are an over-determined system. Least-squares were used to solve for the maximum and minimum principal strains (Equation (2)).

Multiplying the area of the triangle by the strain energy density (Equation (1)) gave the strain energy for a 1 m thick slab located within the triangle.

The energy per meter of thickness is multiplied by the thickness of the crust (taken to be 30 km) to give the total strain energy change in the vertical prism. The 30 km crustal thickness was selected based on the USGS CRUST 5.1 model [15].

4. Results

From the analysis of the ARIA data, the sum of the energy per meter thickness of crust is 5.85×10^{12} J·m². Allowing for a crustal thickness of approximately 30 km, the total energy is 1.75×10^{17} J. This value compares well with the total radiated seismic energy (USGS, 2011) of 1.9×10^{17} Nm (or J). Variations in elastic properties and thickness of the crust would change our total strain energy value, but by less than an order of magnitude.

Although the seismically-observed radiated energy is a useful number, the strain-energy analysis shows the distribution of the sources and sinks of the energy (**Figure 3**) without using a specific earthquake model, e.g., a dislocation model. Some areas of the crust under Japan released energy while some areas may have stored energy. This concept of differential loading and unloading has generally been calculated using a specific model of the faulting [e.g., 21]. From the change in strain the maximum available energy can be determined.

The variation in energy distribution can be seen by

looking at the “cumulative” energy as a function of distance from the trench axis (**Figure 4**).

Figure 3 shows the distribution of strain energy sources and sinks throughout Japan. The green areas represent triangles that increased in area, where the red triangles represent areas of overall shortening.

5. Discussion

5.1. Surface Observations Related to the Whole Crust

An assumption in GPS strain studies is that surface displacements provide information about the elastic response of the entire crustal material. Over the time-scale of the coseismic energy release, a few minutes in duration, the crust can be regarded as a rigid elastic material. By looking at the crustal response over a few minutes, we do not have to consider the longer-term viscous behavior as observed at the year and decade time scales, of the crustal material. Although, the changes in strain over longer time intervals following an earthquake can provide important insights into longer-term crustal deformation and the partitioning of elastic and viscous behaviors, it is not necessary in this study.

The assumption that the surface displacements are representative of the strains throughout the crustal block do appear to be valid because (1) the total energy calculations agree with the independent radiated energy calculation [2], and (2) the March 2011 Tōhoku earthquake hypocenter is put at 30 km depth, which is near the reported base of the upper-plate crust in the study area.

5.2. Influence of Thickness of Continental Crust

A 30 km crustal thickness was used to calculate the total energy released of 1.75×10^{17} J from the strain energy density of 5.85×10^{12} J per meter thickness of material. The total energy released would range from 0.585×10^{17} J for a 10 km thick crust, to 2.93×10^{17} J for a 50 km thick crust. The value changes by a factor of 5, but retains the same order of magnitude as the observed radiated energy. The value of 30 km was derived from the USGS CRUST 5.1 model [15].

5.3. Pre-Earthquake Strain Measurements

Studies of accumulating strain patterns reflects deformation along several tectonic zones over long time periods (earthquakes occurring during the measurement period), whereas in this paper we only consider the effect of a single earthquake along a single segment of a tectonic zone, so reconciling the two patterns is difficult. However, our results indicate that several tectonic zones, which were areas of increased strain accumulation in previous studies, responded to the March 2011 Tōhoku

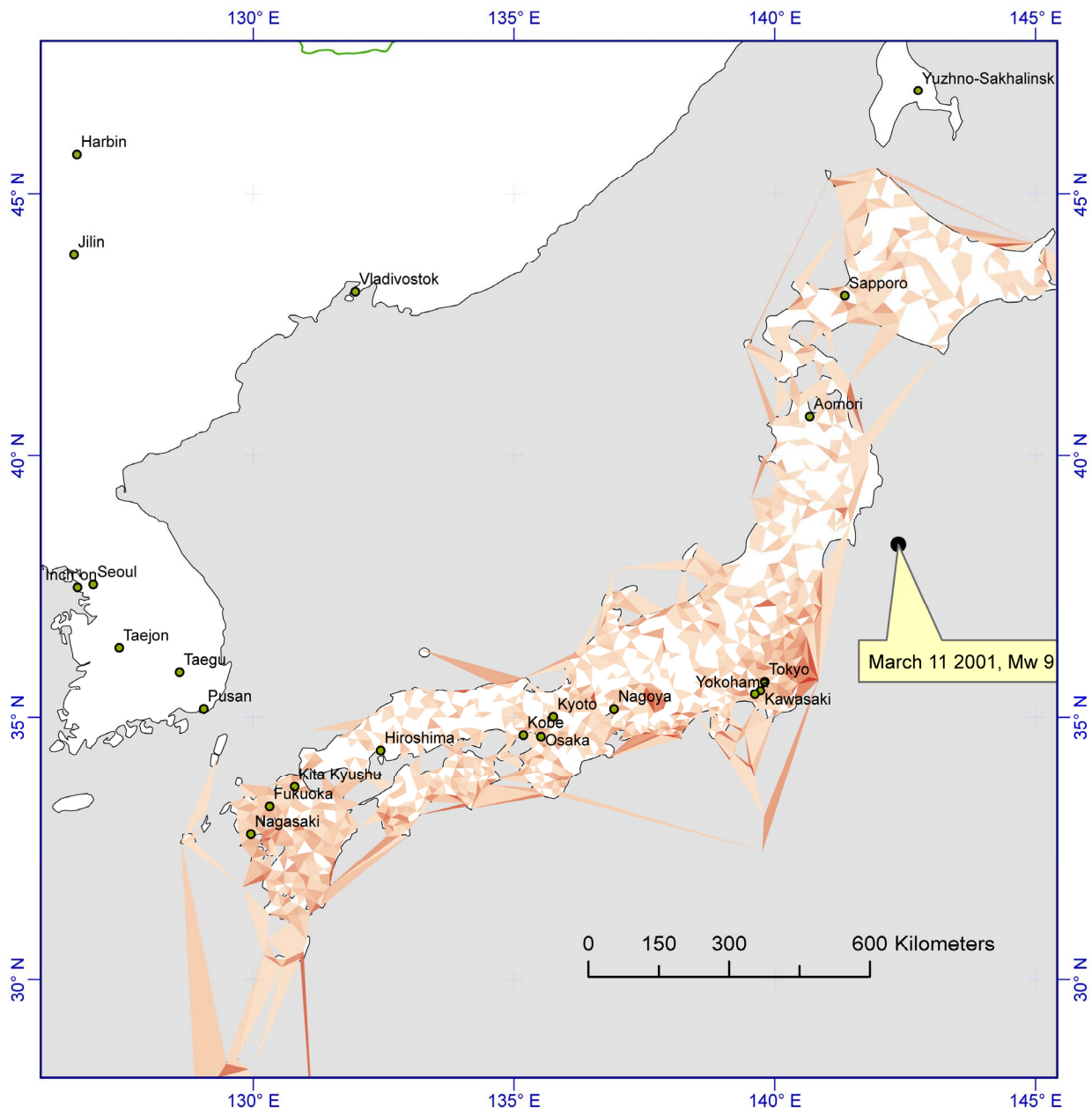


Figure 3. Strain energy density across the Japanese islands. White (land) and grey (oceanic) areas have a very low strain energy density. Darker shading represents greater strain energies. Most of the total energy released is in the large triangles around the epicenter. There is an area of high strain energy density at the southern margin of the rupture zone, just east of Tokyo (Median Tectonic Line, Figure 1). About 5% of the total energy transfer is distributed along the southern coast of Honshu and the West coast of Kyushu (compare with tectonic zones in Figure 1).

earthquake, when and where they became zones of concentrated energy release.

Harada & Simura [6] used three different first-order triangulation surveys conducted over a 94 year range to show the variability in the deformation in areas of Japan. GEONET, which consisted of about 1000 stations at the time, was used by Sagiya and others [16] to look at current crustal deformation in Japan. They concluded that most of the regions of large strain were associated with

tectonic boundaries and volcanoes. GEONET was also used by Hasimoto and others [5] to investigate strain accumulation from a slip-deficit model. All these studies showed that regions of differing amounts of strain coincided with known tectonic zones.

Strain energy release from the 2011 Tōhoku earthquake is shown in **Figure 3**; the denser-colored areas show that the energy density was not uniform across the study area. There is a band of higher strain energy density

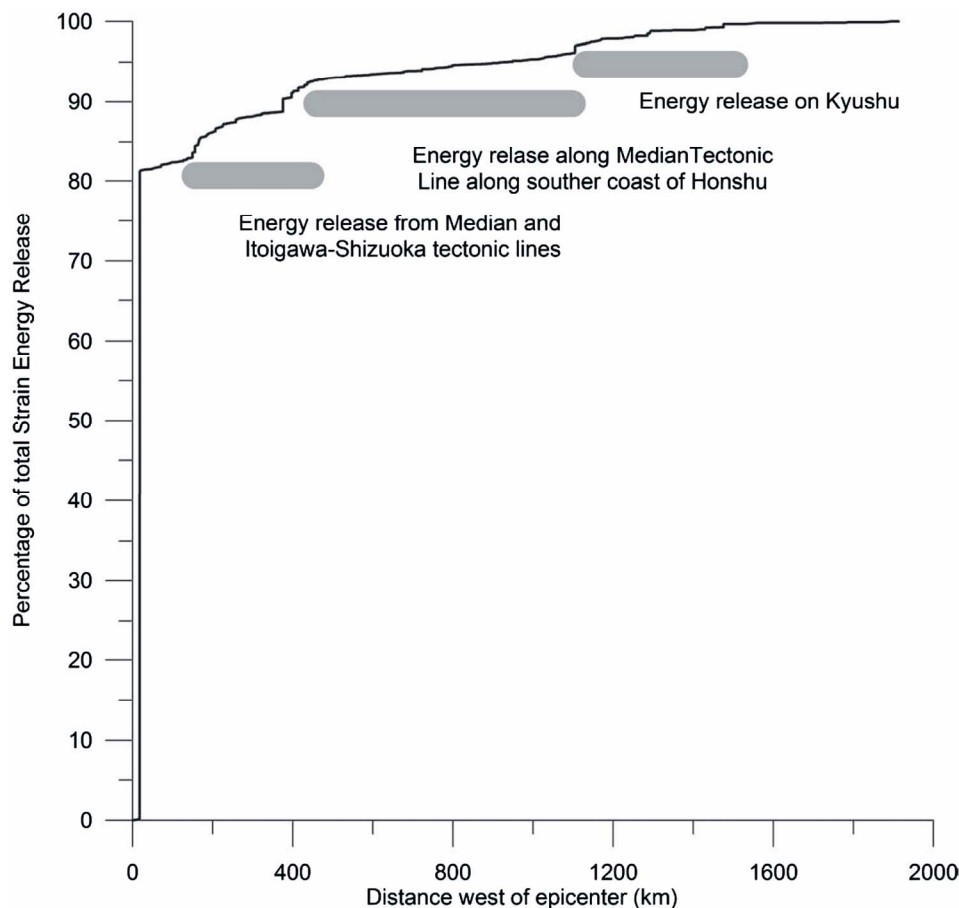


Figure 4. Plot of energy released as a function of distance from the seismic front. The cumulative energy is the total energy released by the entire area of GPS coverage. About 82% of the energy is released within 150 km West of the epicenter. Another 12% is released 150 to 500 km west of the epicenter, and the remaining 6% is released more than 500 km west of the epicenter. The jumps in energy released plot represent the concentrated energy release along tectonic zones.

running WSE-ENE along the southern end of the island of Honshu, which corresponds to the Median Tectonic Line (**Figure 1**). The island of Kyushu, is another area of increased strain energy density, which is at the intersection of the Ryukyu and SW Japan arcs. At the intersection of the Median and Itoigawa-Shizuoka tectonic lines, located just East of Tokyo, is another area of increased strain energy density. Interestingly, the Niigata-Kobe Tectonic Zone, proposed by Sahiya and others [16], does not appear to be a zone of high strain energy density.

Some of the variability in energy release can also be seen by examining **Figure 4**. Eighty-two percent of the energy is released within 150 km west of the epicenter. Between 150 and 500 km west of the epicenter there was rapid increases in total strain energy (a 6% and 4% rise). These abrupt increases in energy release with distance represent the crossing of the Median tectonic line just east of Tokyo and the energy-dense area near Nagoya. The gradual increase of total strain energy from 500 to 1100 km represents the energy released along the Median Tectonic Line (**Figure 1**). There were smaller increases

of 1% - 2% increases approximately 1200 km west of the epicenter, which represent the energy released in the island of Kyushu.

Although the majority of the energy released in the event was close to the epicenter approximately 12% of the total energy was released 150 to 500 km away from the epicenter (**Figure 4**). This 12% accounts for approximately 2.1×10^{16} J of energy, which is the observed radiated seismic energy for a 7.5 M_w earthquake. This landward release of energy could account for some of the reported local strong shaking at substantial distances from the epicenter.

In summary, pre-earthquake strain studies show non-uniform strain accumulation with increased strain accumulation along known tectonic boundaries. These areas of increased strain accumulation showed high-strain energy densities of released elastic strain during the 2011 earthquake. The strain released in the 2011 9.0 M_w Tohoku earthquake shows the same nature of differential strain accumulation as seen by Harada & Simura [6] and Hasimoto and others [5].

6. Conclusions

The 2011 9.0 M_w Tōhoku earthquake provides a unique dataset of displacements over a large area during a subduction zone earthquake. This study used 1204 GPS stations, with an average station-to-station distance of 20 km. GPS data show coseismic displacements for the earthquake using a 9-minute window of data following the earthquake. Displacements from aftershocks are excluded from the dataset, yielding the spatial variability of co-seismic displacements. Some conclusions are:

The amount of strain energy released is the same order of magnitude as the observed radiated seismic energy.

About 12% if the total energy released (energy equivalent to a M_w 7.5 earthquake) was released along tectonic zones across the southern margin of Honshu.

Although energy release occurred throughout the Japanese islands, it is concentrated in known tectonic zones.

The pattern of different areas accumulating versus releasing strain is similar to patterns of strain prior to the 2011 earthquake.

This paper has presented a method for calculating the energy released in an earthquake that 1) is independent of seismic energy methods, and 2) matches the seismically observed radiated energy. This method could be applied to areas that are currently accumulating strain to estimate the amount of potential energy, and thus the magnitude of an earthquake, that the area could generate during megathrust fault rupture.

REFERENCES

- [1] H. F. Reid, "The California Earthquake of April 18, 1906: The Mechanics of the Earthquake," The Carnegie Institution of Washington, Washington, D.C., 1908.
- [2] USGS, US Geological Survey, Vol. 2011, 2011.
- [3] H. Kanamori and E. E. Brodsky, "The Physics of Earthquakes," *Reports on Progress in Physics*, Vol. 67, No. 8, 2004, pp. 1429-1496.
- [4] S. Stein and M. Wysession, "An Introduction to Seismology, Earthquakes, and Earth Structure," Blackwell, Malden, 2003.
- [5] C. Hashimoto, A. Noda, T. Sagiya and M. Matsu'ura, "Interplate Seismogenic Zones along the Kuril-Japan Trench Inferred from GPS Data Inversion," *Nature Geoscience*, Vol. 2, No. 2, 2009, pp. 141-144.
- [6] T. Harada and M. Shimura, "Horizontal Deformation of the Crust in Western Japan Revealed from First-Order Triangulation Carried out Three Times," *Tectonophysics*, Vol. 52, No. 1-4, 1979, pp. 469-478.
- [7] Nuclear Waste Management Organization of Japan, "Evaluating Site Suitability for a HLW Repository (Scientific Background and Practical Application of NUMO's Siting Factors)," *Evaluating Site Suitability for a HLW Repository (Scientific Background and Practical Application of NUMO's Siting Factors)*, Vol. NUMO-TR-04-04, 2004, pp. 29-39.
- [8] J. C. Jaeger, N. G. W. Cook and R. W. Zimmerman, "Fundamentals of Rock Mechanics," Chapman and Hall, London, 2007.
- [9] T. Vincenty, "Direct and Inverse Solutions of Geodesics on the Ellipsoid with Application of Nested Equations," *Survey Review*, Vol. 23, No. 176, 1975, pp. 88-93.
- [10] F. C. Frank, "Deduction of Earth Strains from Survey Data," *Bulletin of the Seismological Society of America*, Vol. 56, No. 1, 1966, pp. 35-43.
- [11] L. E. Malvern, "Introduction to the Mechanics of Continuous Medium," Prentice-Hall, Inc., Englewood Cliffs, 1969.
- [12] K. M. Cruikshank, A. M. Johnson, R. W. Fleming and R. Jones, "Winnetka Deformation Zone. Surface Expression of Coactive Slip on a Blind Fault during the Northridge Earthquake Sequence," Open-File Report No. OF-96-698, 1996, p. 70.
- [13] Y. C. Fung, "Foundations of Solid Mechanics," Prentice-Hall, Englewood Cliffs, 1965.
- [14] T. Hanks and H. Kanamori, "A Moment Magnitude Scale," *Journal of Geophysical Research*, Vol. 84, No. B5, 1979, pp. 2348-2350.
- [15] W. D. Mooney, G. Laske and G. Masters, "CRUST5.1: A Global Crustal Model at 5×5 Degrees," *Journal of Geophysical Research*, Vol. 103, 1998, pp. 727-747.
- [16] T. Sagiya, S. I. Miyazaki and T. Tada, "Continuous GPS Array and Present-Day Crustal Deformation of Japan," *Pure and Applied Geophysics*, Vol. 157, No. 11-12, 2000, pp. 2303-2322.
- [17] G. Plafker, "Tectonics of the March 27, 1964 Alaska Earthquake," Professional Paper No. 543-I, 1969, p. 74.
- [18] G. Plafker, "Alaskan Earthquake of 1964 and Chilean Earthquake of 1960: Implications for Arc Tectonics," *Journal of Geophysical Research*, Vol. 77, No. 5, 1972, pp. 901-925.
- [19] ARIA, "Preliminary GPS Time Series Provided by the ARIA (Advanced Rapid Imaging and Analysis) Team at JPL and Caltech," 2011. <ftp://sideshow.jpl.nasa.gov/pub/usr/ARIA/>
- [20] B. Delaunay, "Sur la Sphère Vide," *Otdelenie Matematicheskikh i Estestvennykh Nauk*, Vol. 7, 1934, pp. 793-800.
- [21] G. C. P. King, R. S. Stein and J. Lin, "Static Stress Changes and the Triggering of Earthquakes," *Bulletin of the Seismological Society of America*, Vol. 84, No. 3, 1994, pp. 935-953.